Journal of ELECTRONIC MATERIALS, Vol. 49, No. 6, 2020
https://doi.org/10.1007/s11664-020-08106-w

Experimental, Semi-theoretical, and Theoretical Electronic and Non-linear Optical Characteristics of ECBP

EMİNE TANIŞ,[1,5] EMİNE BABUR SAS,[2] BAYRAM GÜNDÜZ,[3] and MUSTAFA KURT[4]

1.—Department of Medical Services and Techniques, Vocational School of Health Services, Kırşehir Ahi Evran University, 40100 Kırşehir, Turkey. 2.—Department of Electronics and Automation, Vocational School of Technical Sciences, Kırşehir Ahi Evran University, 40100 Kırşehir, Turkey. 3.—Department of Science Education, Faculty of Education, Muş Alparslan University, 49250 Muş, Turkey. 4.—Department of Biophysics, Faculty of Medicine, Kırşehir Ahi Evran University, 40100 Kırşehir, Turkey. 5.—e-mail: eminetanis@ahievran.edu.tr

The electronic properties of 4,4′-bis(3-ethyl-*N*-carbazolyl)-1,1′-biphenyl (ECBP) have been studied using time-dependent density functional theory. The non-linear optical (NLO) properties and dipole moments were investigated to understand the optical behavior of ECBP. Frontier molecular orbitals were determined to define the energetic properties of the title molecule. The total density of states, partial density of states, and overlap population electronic density of states of ECBP were calculated and analyzed. Experimental and semi-theoretical parameters such as the optical density, transmittance, absorbance band edge, optical bandgap, refractive index, incidence angle, and refraction angle of ECBP at 3 mM, 10 mM, 21 mM, and 70 mM were obtained. The results indicate that this molecule is a suitable material for NLO, optical, and optoelectronic devices.

Key words: ECBP molecule, optoelectronic devices, experimental, semi-theoretical and theoretical studies, electronic and non-linear optical properties

INTRODUCTION

Organic semiconductors have attracted considerable interest over the last few years due to their low cost, flexibility, and potential use in large-scale organic devices including electronic, optoelectronic, and organic photovoltaic devices,[1] organic light-emitting diodes,[2,3] sensors,[4–9] photodetectors,[10] transistors,[11] radiofrequency identification tags,[12] and large-area integrated circuits.[13] They are also promising for use in solid-state lighting including efficient white organic light-emitting devices (WOLEDs).[14,15] Carbazole-based host materials are often used in WOLED applications.[16–20] Carbazole-based organic semiconducting derivatives are promising host materials because of their rigid molecular structure, close highest occupied molecular orbital (HOMO) and lowest unoccupied molecular orbital (LUMO) energy levels, hole transport properties, and restricted backward energy transfer.[21] Examples of these are polymers such as 4,4′-bis(*N*-carbazolyl)-1,1′-biphenyl, 4,4′-bis(9-carbazolyl)-1,1′-biphenyl (CBP) and poly(vinylcarbazole).[22–27] 4,4′-Bis(3-ethyl-*N*-carbazolyl)-1,1′-biphenyl (ECBP) molecule, a carbazole derivative, can be obtained by adding electron-rich CH_3 groups to the ends of the CBP molecule. These two ethyl groups are expected to modify the HOMO and LUMO energy levels as well as the electronic and optic properties.

In recent years, theoretical calculations have been important in terms of throwing light on the electronic, optical, and structural properties of organic semiconductors for comparison with experimental results.[28–30] In the work presented herein, the electronic and optical properties of ECBP, a carbazole-derived organic light-emitting diode and host

(Received December 20, 2019; accepted March 21, 2020; published online April 6, 2020)

material, were investigated. To the best of the authors' knowledge, no studies on the electronic and optical behavior of this molecule are available. The electronic and optical properties of the title material were analyzed in detail for various solvents and concentrations. Theoretically, the excitation energies, HOMO–LUMO energy levels, and bandgap between these energy levels were calculated by using time-dependent density functional theory (TD-DFT). Also, the NLO properties and total density of states (TDOS) or DOS, partial density of states (PDOS), overlap population electronic density of states (OPDOS) or COOP, and the group contributions of molecular orbitals were calculated and are discussed in detail. The experimental results were compared with the theoretical and semi-theoretical values.

EXPERIMENTAL PROCEDURES

Materials

4,4′-Bis(3-ethyl-*N*-carbazolyl)-1,1′-biphenyl (ECBP) organic molecule and chloroform and dimethylformamide (DMF) as solvents were obtained from Sigma-Aldrich. Figure 1a, b, and c show the two-dimensional (2D), three-dimensional (3D), and theoretical optimized geometric structures of the ECBP molecule, respectively.

ECBP Solutions

We weighed amounts of ECBP to achieve concentrations of 3 mM, 10 mM, 21 mM, and 70 mM using an AND-GR-200 series analytical balance. The amounts of ECBP were dissolved in DMF solvent using a digital vortex mixer (Four E's Scientific CO., Ltd.).

UV Spectrophotometry

Optical measurements were carried out on 3 mM, 10 mM, 21 mM, and 70 mM ECBP solutions using a UV-1800 spectrophotometer (Shimadzu) at room temperature.

COMPUTATIONAL DETAILS

All theoretical calculations were performed by the TD-DFT method using the Gaussian 09 program package[31] at B3LYP[32] and CAM-B3LYP level.[33] In literature, the results obtained using the CAM-B3LYP functional for some molecular structures are more reliable than those obtained using the B3LYP functional.[33–35] Therefore, to confirm the accuracy of the presented calculations, excitation energies were calculated using both the B3LYP and CAM-B3LYP functionals and compared with the experimental results. The electronic and NLO properties of the optimized molecule were calculated. The theoretically obtained E_g values were compared with the experimental value. The GaussSum 2.2 program[36] was used to analyze the TDOS or DOS, PDOS, OPDOS or COOP, and group contributions of molecular orbitals.

RESULTS AND DISCUSSION

Experimental Results

The absorbance or optical density spectra of ECBP at 3 mM, 10 mM, 21 mM, and 70 mM are

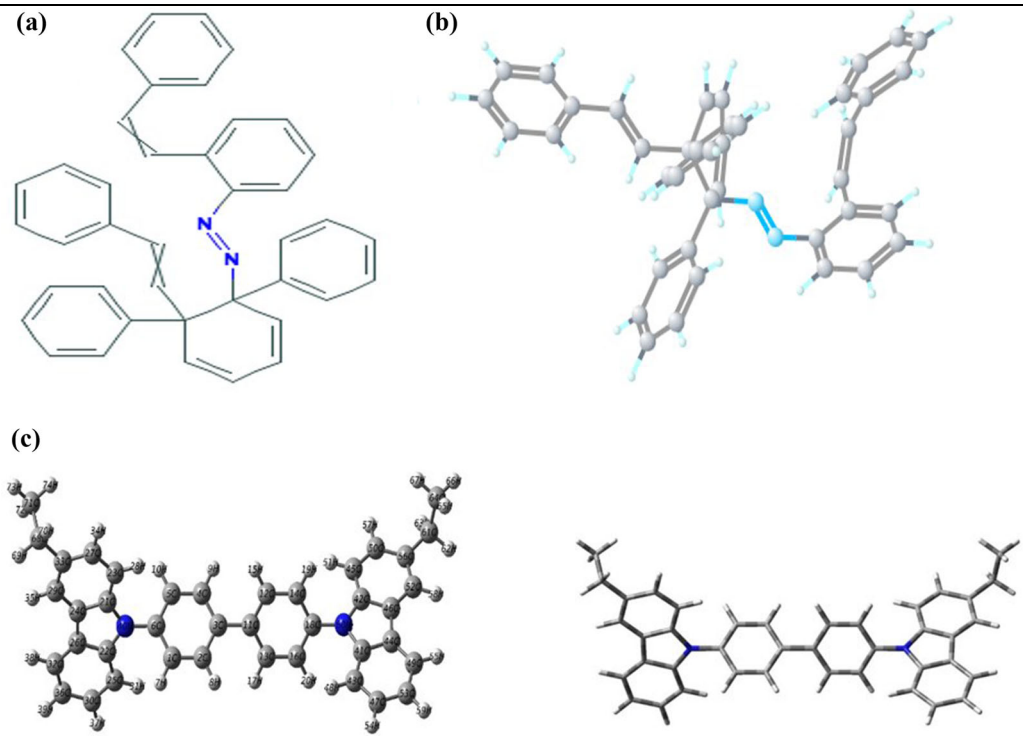

Fig. 1. (a) 2D, (b) 3D, and (c) theoretical optimized geometric structures of 4,4′-bis(3-ethyl-*N*-carbazolyl)-1,1′-biphenyl (ECBP).

shown in Fig. 2. As seen in Fig. 2, the entire absorbance curve of ECBP at 70 mM was not observed due to the nature of the device.[37] The absorption spectra of ECBP at 3 mM and 10 mM showed maximum peaks at 240 nm and 241 nm, respectively. Furthermore, ECBP also showed smaller peaks and hollow structure characteristics at the respective wavelengths as shown in the figure. As seen, the spectra of ECBP remained constant at the lowest values at wavelengths longer than about 380 nm. These results suggest that the absorption spectra of ECBP reach their highest values in the near-ultraviolet (NUV) region of the absorption spectrum; i.e., they are dominant in this region.

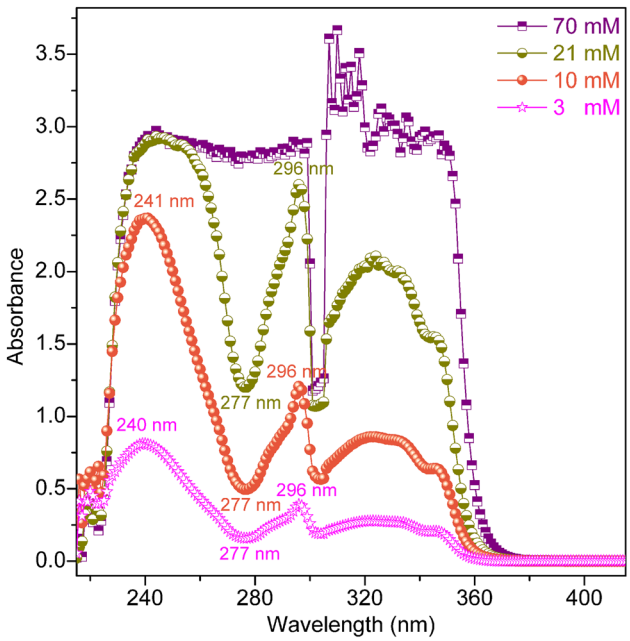

Fig. 2. Absorbance spectra of ECBP at 3 mM, 10 mM, 21 mM, and 70 mM.

The transmittance (T) is an important parameter among the optical properties. Figure 3a shows the transmittance spectra of ECBP at 3 mM, 10 mM, 21 mM, and 70 mM. As seen in Fig. 3a, the transmittance spectra of ECBP exhibited various peak and pit characteristics in the NUV region, but remained constant at the maximum values in the visible (V) region. In the NUV region, the absorption values of ECBP increased as the concentration was increased while the transmittance values decreased. These results are expected and consistent with similar studies. The absorbance band edge ($E_{\text{Abs-be}}$) provides important information about the spectroscopic and electronic structure. The $E_{\text{Abs-be}}$ values of ECBP at 3 mM, 10 mM, 21 mM, and 70 mM were found from the maximum peaks using the curves of $dT/d\lambda$ versus wavelength (λ) as seen in Fig. 3b and presented in Table I. Table I reveals that the $E_{\text{Abs-be}}$ value of ECBP decreased from 3.388 eV to 3.255 eV with increasing concentration.

The optical bandgap (E_g) is a fundamental optical parameter and can be obtained from the Tauc model.[38] Firstly, having determined the type[37,39] of optical transition, the allowed direct bandgap (E_{gd}) was found to be suitable for ECBP. Figure 4 shows the $(\alpha h\vartheta)^2$ versus photon energy (E) curves for ECBP at 3 mM, 10 mM, 21 mM, and 70 mM. The E_{gd} values of ECBP at 3 mM, 10 mM, 21 mM, and 70 mM were obtained by extrapolating the linear plot to $(\alpha h\vartheta)^2 = 0$ and are presented in Table I. The allowed direct bandgap of ECBP decreased from 3.441 eV to 3.316 eV with increasing concentration.

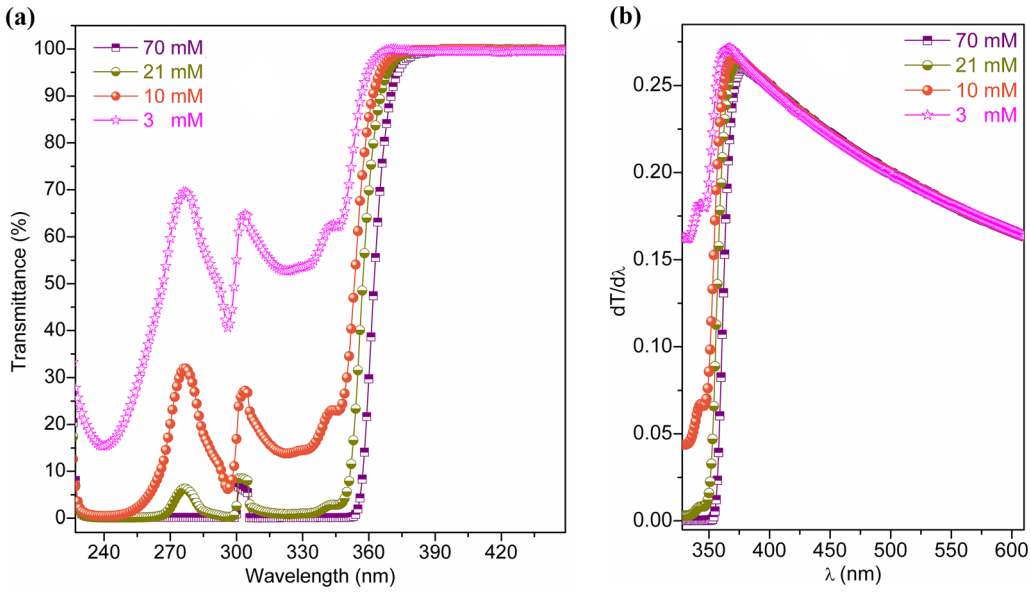

Fig. 3. (a) Transmittance spectra and (b) $dT/d\lambda$ versus wavelength (λ) curves of ECBP at 3 mM, 10 mM, 21 mM, and 70 mM.

These optical bandgap values indicate that ECBP exhibited semiconducting property.

The refractive index of ECBP at 3 mM, 10 mM, 21 mM, and 70 mM was obtained using various relations such as those of Herve-Vandamme, Kumar-Singh, Moss, Ravindra, and Reddy[30,40] and are presented in Table IIa, revealing an increase with increasing concentration. The lowest refractive index was observed for the Ravindra relation, while the highest refractive index was observed for the Reddy relation. The average refractive index of ECBP increased from 2.274 to 2.311 with increasing concentration.

Table I. Absorption band edge ($E_{Abs\text{-}be}$) and optical bandgap (E_g) of ECBP at 3 mM, 10 mM, 21 mM, and 70 mM

Concentration	$E_{Abs\text{-}be}$ (eV)	E_g (eV)
3	3.388	3.441
10	3.333	3.395
21	3.316	3.363
70	3.255	3.316

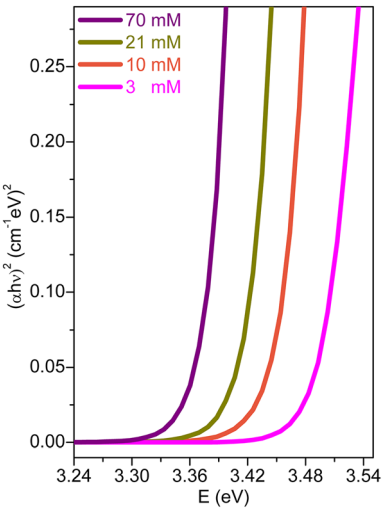

Fig. 4. $(\alpha h\vartheta)^2$ versus photon energy (E) curves for ECBP at 3 mM, 10 mM, 21 mM, and 70 mM.

The refractive index provides important information on the angles of incidence (Φ_1) and refraction (Φ_2). The Φ_1 and Φ_2 values for ECBP at 3 mM, 10 mM, 21 mM, and 70 mM were obtained respectively from the following equations:[41–43]

$$\Phi_1 = \tan^{-1}\left(\frac{n_2}{n_1}\right) \quad (1)$$

and

$$\Phi_2 = \sin^{-1}\left(\frac{n_1}{n_2}\sin\Phi_1\right). \quad (2)$$

Figure 5 shows plots of Φ_1 and Φ_2 versus E for ECBP at 3 mM, 10 mM, 21 mM, and 70 mM. The upper curves correspond to the angle of incidence, while the bottom curves indicate the refraction angle. Φ_1 and Φ_2 vary with the angular frequency (from about 4.9 Hz to 8.4 Hz). On the other hand, the angle of incidence of ECBP increased with increasing concentration, while the refraction angle decreased.

Semi-theoretical Results

In this section, we discuss the theoretical molar absorptivity values (see "Computational Details" section for details) and the other parameters obtained from the molar absorptivity. Figure 6a indicates the molar absorptivity and transmittance spectra of ECBP. The molar absorptivity spectra of ECBP exhibit peaks at 237 nm, 263 nm, and

Table II. (a) Experimental and (b) semi-theoretical refractive indices of ECBP obtained from the Moss, Ravindra, Herve-Vandamme, Reddy, and Kumar-Singh relations and their average

	Refractive Index (n)					
Concentration	Moss	Ravindra	Herve-Vandamme	Reddy	Kumar-Singh	Average
(a)						
3	2.292	1.951	2.207	2.660	2.261	2.274
10	2.300	1.979	2.219	2.670	2.270	2.288
21	2.305	1.999	2.227	2.677	2.277	2.297
70	2.314	2.028	2.240	2.688	2.288	2.311

Refractive index (n)					
Moss	Ravindra	Herve-Vandamme	Reddy	Kumar-Singh	Average
(b)					
2.208	1.607	2.078	2.552	2.154	2.120

288 nm (the highest peak) and pits at 249 nm and 273 nm. The transmittance spectra of ECBP exhibit peaks at 249 nm and 273 nm and remain constant at wavelengths longer than about 315 nm. The transmittance of ECBP increased very sharply from about 295 nm to 315 nm (Fig. 6a). Like the experimentally obtained results, the theoretically obtained absorbance spectra are more dominant in the NUV region. The semi-theoretical $E_{\text{Abs-be}}$ value of ECBP was obtained from the maximum peaks using the $dT/d\lambda$ versus λ curves as seen in Fig. 6b and found to be 3.936 eV. This semi-theoretical $E_{\text{Abs-be}}$ value is higher than the experimental $E_{\text{Abs-be}}$ values.

To obtain a semi-theoretical E_{gd} value for ECBP, $(\alpha h\vartheta)^2$ is plotted versus E in Fig. 7. The E_{gd} value of ECBP was found to be 3.996 eV. This semi-theoretical E_{gd} value is higher than the experimental E_{gd} values. On the other hand, the semi-theoretical optical bandgap indicates that the optical bandgap of ECBP lies at the limit of semiconductors.

The semi-theoretical refractive indices of ECBP were obtained using the Herve-Vandamme, Kumar-Singh, Moss, Ravindra, and Reddy relations and are presented in Table IIb. As seen in Table IIb, the lowest refractive index (1.607) was observed for the Ravindra relation, while the highest refractive index (2.552) was observed for the Reddy relation. The average refractive index of ECBP was 2.120. These semi-theoretical refractive indices are lower than the experimental values.

The semi-theoretical Φ_1 and Φ_2 values of ECBP were obtained using Eq. (1) and (2), respectively.

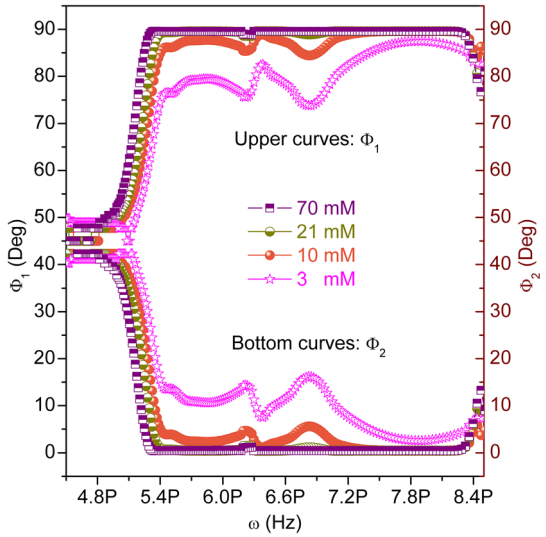

Fig. 5. Angles of incidence (Φ_1) and refraction (Φ_2) curves of ECBP at 3 mM, 10 mM, 21 mM, and 70 mM.

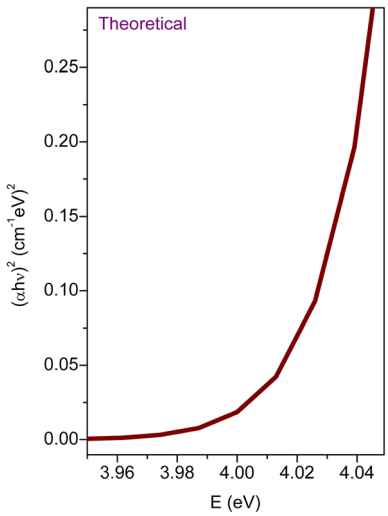

Fig. 7. $(\alpha h\vartheta)^2$ versus E curves of ECBP to obtain the semi-theoretical optical bandgap.

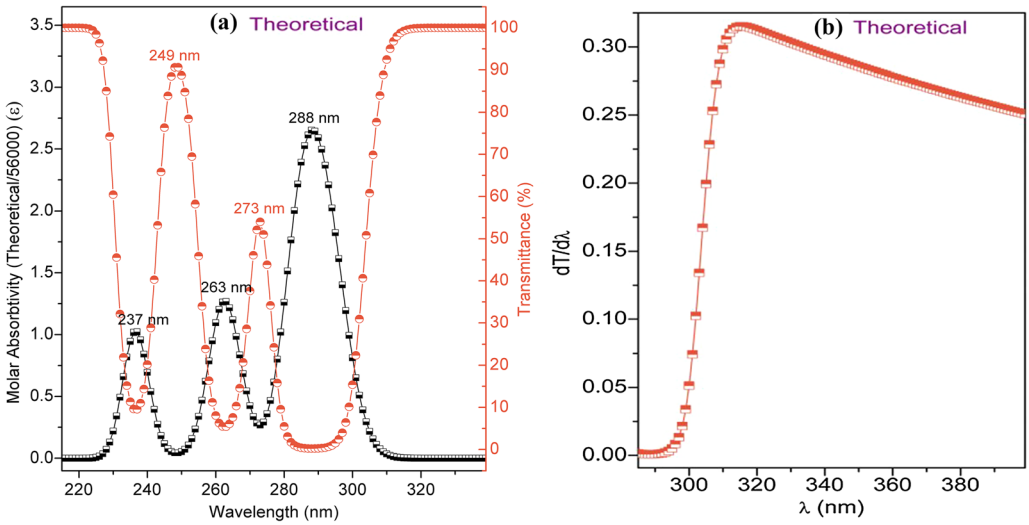

Fig. 6. (a) Absorbance and transmittance spectra and (b) $dT/d\lambda$ versus λ curves of ECBP at 3 mM, 10 mM, 21 mM, and 70 mM.

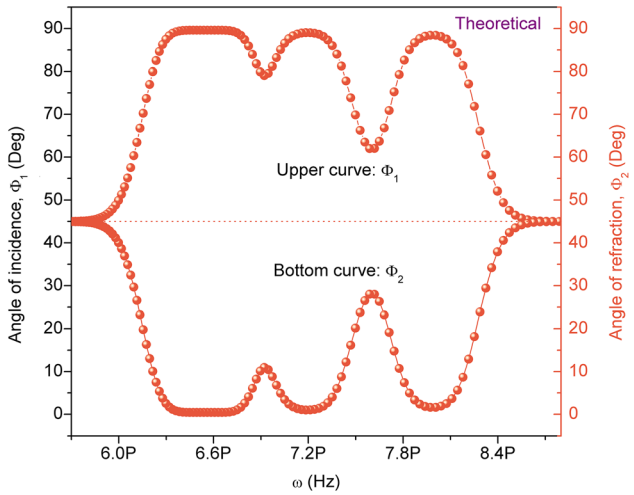

Fig. 8. Semi-theoretical angles of incidence (Φ_1) and refraction (Φ_2) curves of ECBP.

Figure 8 shows the Φ_1 and Φ_2 versus E curves of ECBP. The upper curve corresponds to the angle of incidence, while the bottom curve shows the refraction angle. Φ_1 and Φ_2 vary with the angular frequency (from about 5.9 Hz to 8.5 Hz). The semi-theoretical angles of incidence are higher than the semi-theoretical refraction angles.

Theoretical Results

Ultraviolet–Visible Spectroscopy

The UV–Vis absorption spectrum of the material calculated by the CAM-B3LYP method in chloroform as solvent is shown in Fig. 6a, revealing three dominant peaks at 237 nm, 263 nm, and 288 nm when using this method. Meanwhile, the absorption bands were calculated at 321 nm and 349 nm when using the B3LYP method. Experimentally, two peaks were observed in chloroform, at 241 nm and 296 nm. These results confirm that the UV–Vis absorption spectrum obtained using the CAM-B3LYP method are more consistent with the experimental results.

Frontier Molecular Orbitals

The E_g values in chloroform as solvent were calculated as 4.11 eV when using the B3LYP method and 6.56 eV when using the CAM-B3LYP method. The experimental E_g value was found as 3.39 eV in chloroform as solvent. Comparing the calculated E_g values with the measured E_g results reveals that the B3LYP method (4.11 eV) have a better result than the CAM-B3LYP method (6.56 eV) (Fig. 7).

The energies of the frontier molecular orbitals (FMOs) were calculated using the B3LYP/6-311G(d,p) method in gas phase, revealing 143 as the HOMO orbital. The HOMO–LUMO shapes for the molecule in gas phase are shown in Fig. 9. The HOMO orbitals or valence band were spread over

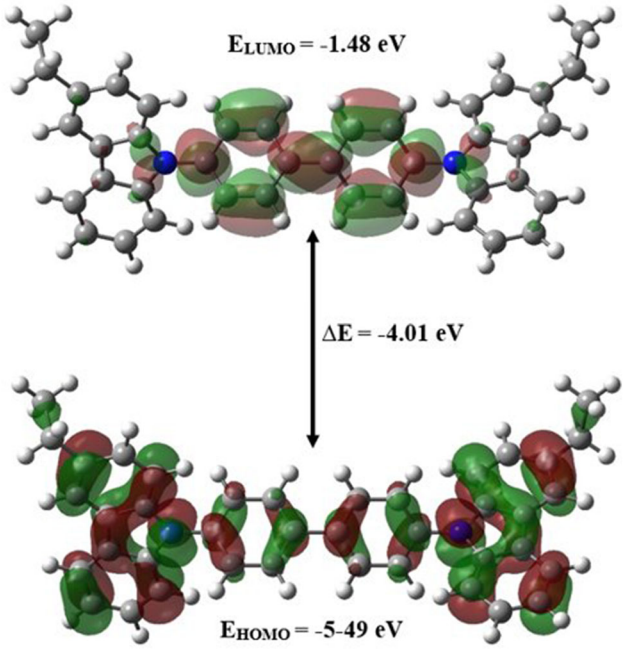

Fig. 9. Frontier molecular orbitals of ECBP in gas phase.

the whole molecule, while the LUMO orbitals or conductivity band were spread over the phenyl ring. Moreover, it appears that the carbazole groups in this molecule make little contribution to the conductivity band. The energy gap, i.e., the energy difference between the HOMO and LUMO orbitals, is an important parameter for evaluating the conductivity and reactivity. As seen in Fig. 9, this value (4.01 eV) was the same in the gas phase.

The HOMO–LUMO energy range is not sufficient to determine the polarizability value, which is an important criterion for the non-linear optical properties of the molecule. Because the CH_3 donor groups at the ends of the CBPE molecule increase the value of the charge symmetry of the molecule's base charge and its first-order hyperpolarizability, the molecule can be considered to be a non-linear optical material.

NLO Analysis

NLO materials have extensive application areas such as storage, optical switching, communication, optical sensors, displays, and signal processing.[44–46] Theoretical calculations can provide sufficient and reliable results to investigate new non-linear materials. In this study, the electrical dipole moment (μ), hyperpolarizability (β), and polarizability (α) were calculated as NLO properties using the B3LYP/6-311++G(d,p) basis set to understand the optical and electrical response of ECBP. The molecular α and β tensors were provided via a Gaussian output file, and its atomic units (a.u.) were converted to electronic units (esu) (1 a.u = 0.1482×10^{-24} esu for α; 1 a.u. = 8.6393×10^{-33} esu for β). The values of the mean polarizability (α), anisotropy of polarizability

($\Delta\alpha$), mean molecular hyperpolarizability ($<\beta>$), and total dipole moment (μ_{tot}) were calculated using the following equations:

$$\alpha_{tot} = \frac{1}{3}(\alpha_{xx} + \alpha_{yy} + \alpha_{zz}), \quad (3)$$

$$\Delta\alpha = \frac{1}{\sqrt{2}}\left[(\alpha_{xx} - \alpha_{yy})^2 + (\alpha_{yy} - \alpha_{zz})^2 + (\alpha_{zz} - \alpha_{xx})^2 + 6\alpha_{xz}^2 + 6\alpha_{xy}^2 + 6\alpha_{yz}^2\right]^{\frac{1}{2}}, \quad (4)$$

$$\langle\beta\rangle = \left[(\beta_{xxx} + \beta_{xyy} + \beta_{xzz})^2 + (\beta_{yyy} + \beta_{yzz} + \beta_{yxx})^2 + (\beta_{zzz} + \beta_{zxx} + \beta_{zyy})^2\right]^{\frac{1}{2}}, \quad (5)$$

$$\mu_{tot} = \left(\mu_x^2 + \mu_y^2 + \mu_z^2\right)^{\frac{1}{2}}. \quad (6)$$

The calculated values are presented in Table III. As organic light-emitting diodes rely on optically active materials, the NLO properties are important to interpret the optoelectronic response.

For a molecule to behave like a good NLO material, the β, μ, and $\Delta\alpha$ must be large. The magnitude of these values is generally interpreted relative to the values of urea. In this study, the values of β_{tot} and $\Delta\alpha$ were calculated to be $3150.816685 \times 10^{-33}$ esu and $199.7953356 \times 10^{-24}$ esu, respectively, compared with $\beta_{tot} = 194.7 \times 10^{-33}$ esu and $\Delta\alpha = 3.8312 \times 10^{-24}$ esu for urea. It is seen that the β_{tot} value of ECBP is approximately 16 times higher than that of urea, and similarly the $\Delta\alpha$ is about 52 times larger. These results show that ECBP could be used as a high-NLO material in future applications.

Table III. Dipole moment μ (D), polarizability α (a.u.), average polarizability α_o ($\times 10^{-24}$ esu), anisotropy of polarizability $\Delta\alpha$ ($\times 10^{-24}$ esu), and first hyperpolarizability β ($\times 10^{-33}$ esu)

μ_x	−0.0003	β_{xxx}	12.4418
μ_y	0.425	β_{xxy}	1492.9641
μ_z	−0.0001	β_{xyy}	−25.6564
μ_0	0.425000118	β_{yyy}	1771.9187
α_{xx}	110.892768	β_{xxz}	−11.1735
α_{xy}	−0.028259	β_{xyz}	−4353.4629
α_{yy}	70.735884	β_{yyz}	2.0410
α_{xz}	0.940332	β_{xzz}	24.2011
α_{yz}	−0.063325	β_{yzz}	−114.0939
α_{zz}	48.186562	β_{zzz}	1.7151
α_{total}	76.605071	β_x	10.9865477
$\Delta\alpha$	199.7953356	β_y	3150.7888
		β_z	−7.417434298
		β	3150.816685

Total, Partial, and Population Density of States (DOS, PDOS, and OPDOS)

Because molecular orbitals with nearby energies in the boundary regions of a molecule may be semidegenerate, it may not be sufficient to consider only the HOMO and LUMO when defining the molecular boundary orbital.[47] In this regard, the TDOS, PDOS, and OPDOS (or COOP) density of states[48–50] were calculated and constructed using the GaussSum2.2 program by convolving the molecular orbital information with Gaussian curves of unit height and full-width at half-maximum (FWHM) of 0.3 eV. TDOS, PDOS, and OPDOS graphs are presented in Figs. 10, 11, 12, and 13. Positive, negative, and zero values in the OPDOS diagram indicate interactions with bonding, antibonding, and nonbonding character, respectively.[50] In addition, the OPDOS diagram helps to identify orbitals that are binding and nonbinding and at the same time determine the donor–acceptor properties of the molecule. Figure 9 reveals that the phenyl rings make the greatest contribution to the frontier molecular orbitals. Figure 10 illustrates some of the orbital energy values of the interactions among the selected groups. Since the ECBP molecule is symmetric in structure, it is seen in Fig. 10 that the orbital energy values of the groups formed by the N60 and N40 carbazole groups are overlapping. The interactions among the carbazole N60 and carbazole N40 groups are zero, indicating nonbinding orbitals.

CONCLUSIONS

The electronic, optical, and non-linear optical properties of ECBP, a carbazole-based organic semiconductor, were investigated by both experimental and theoretical methods. TD-DFT calculations were performed to obtain the UV–Vis

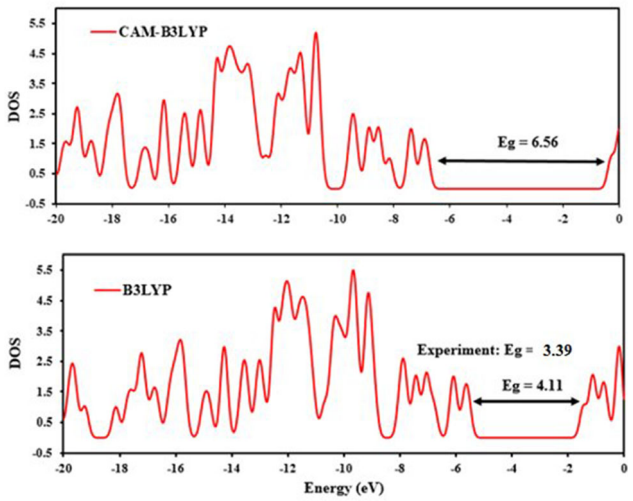

Fig. 10. Density of states (DOS) spectrum (using B3LYP and CAM-B3LYP functionals) of ECBP in chloroform obtained from Mulliken population analysis.

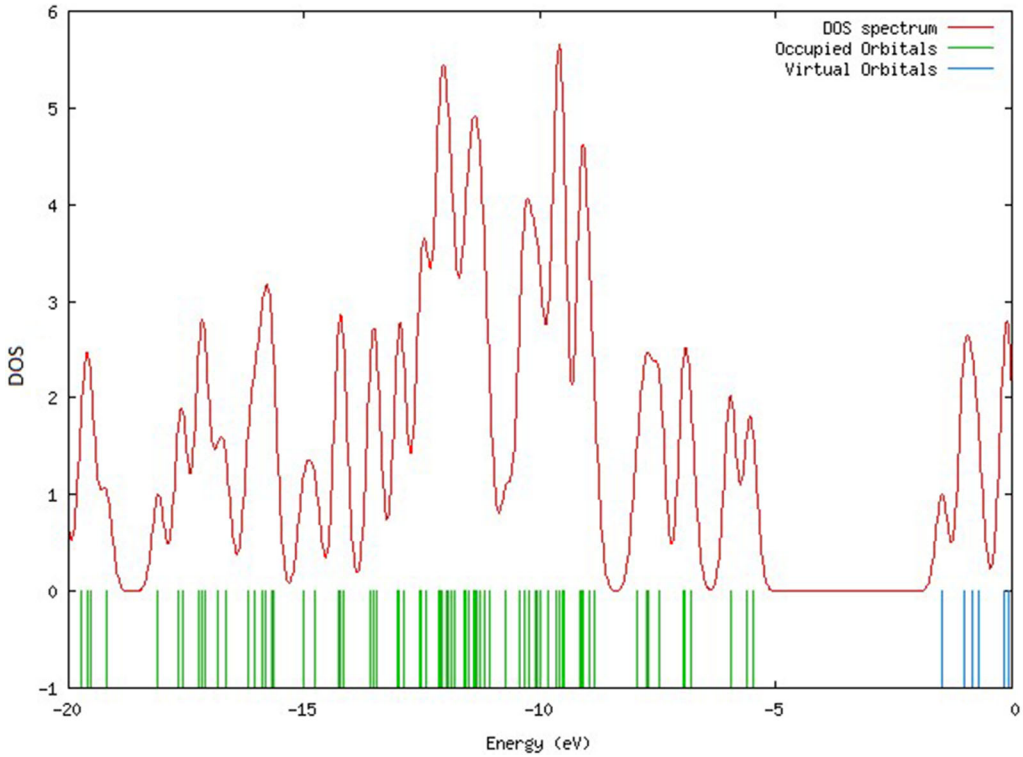

Fig. 11. Total electronic density of states (TDOS) diagram of ECBP.

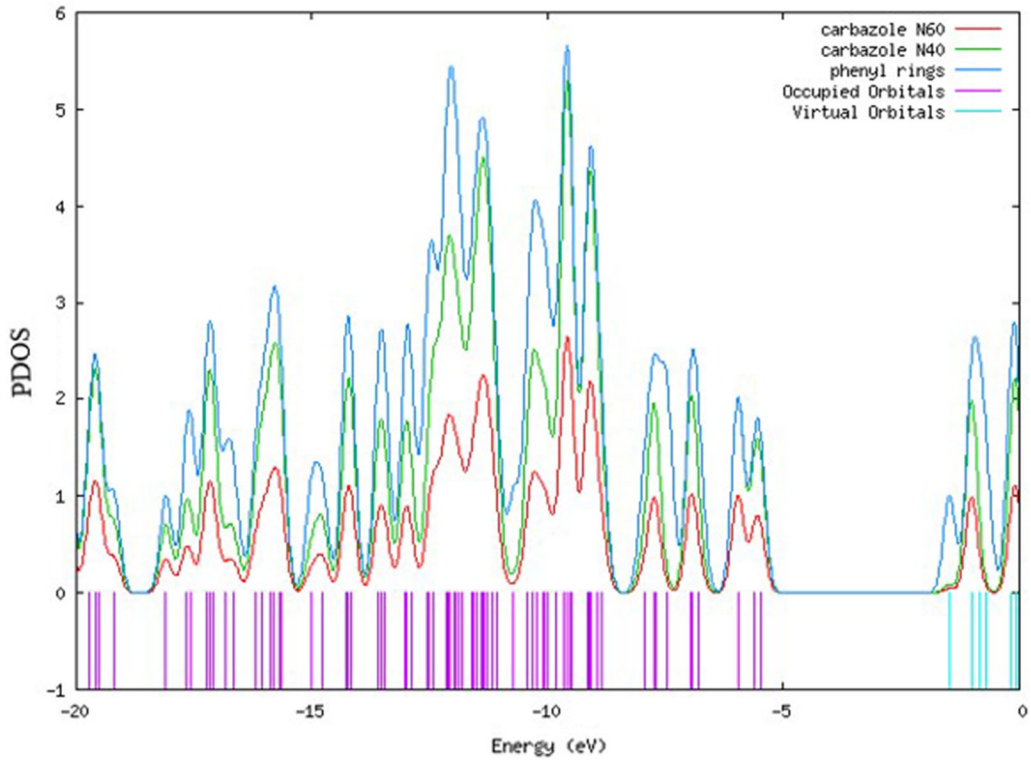

Fig. 12. Partial electronic density of states (PDOS) diagram of ECBP.

spectrum of ECBP. FMO analysis and physicochemical properties were calculated at the same theory of level in chloroform and gas phase. Furthermore, the β, μ, and $\Delta\alpha$ values of the title molecule were obtained. The β value of ECBP was calculated to be 16 times higher than that of urea

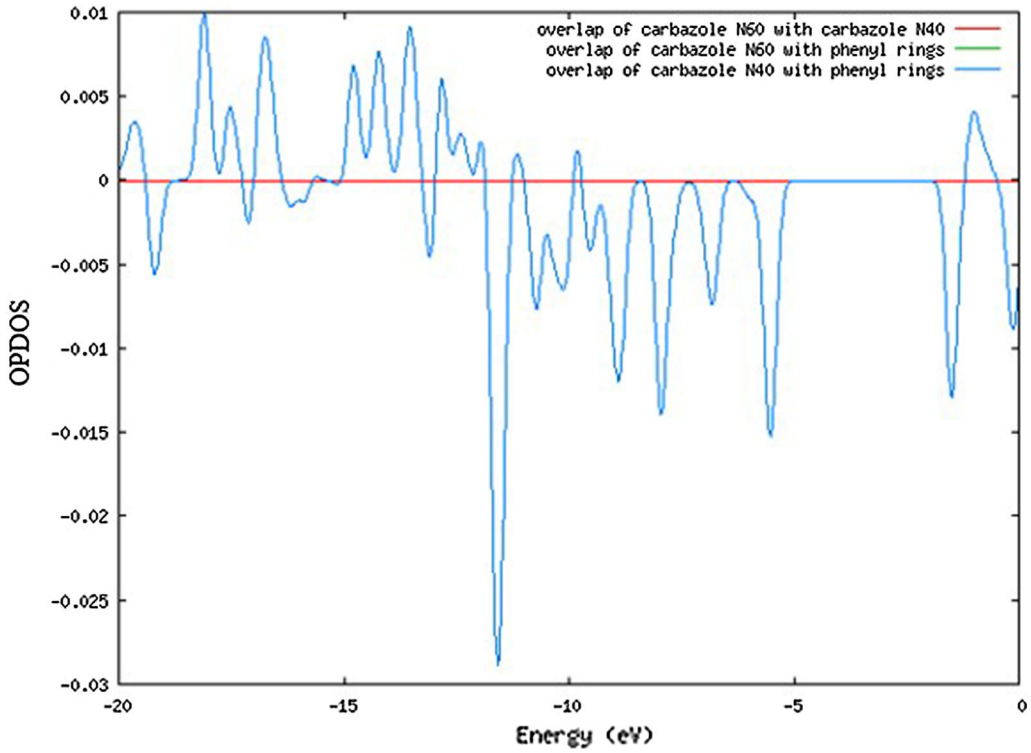

Fig. 13. Overlap population electronic density of states (OPDOS) diagram of ECBP.

($\beta = 0.37 \times 10^{-30}$ esu) while the $\Delta\alpha$ value was 52 times greater than that of urea ($\Delta\alpha = 3.83 \times 10^{-24}$ esu). These results indicate that ECBP could be a good NLO material. The experimental absorbance band edge of ECBP decreased from 3.388 eV to 3.255 eV with increasing concentration. The semi-theoretical absorbance band edge and allowed optical bandgap of ECBP were higher than the experimental values. The semi-theoretical refractive indices were lower than the experimental values. ECBP exhibited semiconducting property.

ACKNOWLEDGMENTS

This work was supported by Kırşehir Ahi Evran University Scientific Project Unit (BAP) through Project No. PYO–FEN.4001.15.012.

CONFLICT OF INTEREST

The authors declare they have no conflicts of interest.

REFERENCES

1. A.A.M. Farag, B. Gunduz, F. Yakuphanoglu, and W.A. Farooq, *Synth. Met.* 160, 2559–2563 (2010).
2. B. Gunduz, I.S. Yahia, and F. Yakuphanoglu, *Microelectron. Eng.* 98, 41–57 (2012).
3. M.Y. Ameen, T. Abhijith, D. Susmita, S.K. Ray, and V.S. Reddy, *Org. Electron.* 14, 554–559 (2013).
4. F. Aziz, M.H. Sayyad, K. Sulaiman, B.Y. Mailis, K.S. Karimov, Z. Ahmad, and G. Sugandi, *Meas. Sci. Technol.* 23, 014001–014009 (2012).
5. M. Murugavelu, P.K.M. Imran, K.R. Sankaran, and S. Nagarajan, *Mater. Sci. Semicond. Process.* 16, 461–466 (2013).
6. G. Harsaanyi, *Sens. Rev.* 20, 98–105 (2000).
7. Y. Che, X. Yang, G. Liu, C. Yu, H. Ji, J. Zuo, J. Zhao, and L. Zang, *J. Am. Chem. Soc.* 132, 5743–5750 (2010).
8. Y. Huang, R. Yuan, and S. Zhou, *J. Mater. Chem.* 22, 883–888 (2012).
9. Y. Huang, L. Fu, W. Zou, and F. Zhang, *New J. Chem.* 36, 1080–1084 (2012).
10. J.B. Wang, W.L. Li, B. Chu, C.S. Lee, Z.S. Su, G. Zhang, S.H. Wu, and F. Yan, *Org. Electron.* 12, 34–38 (2011).
11. H.R. Tseng, H. Phan, C. Luo, M. Wang, L.A. Perez, S.N. Patel, L. Ying, E.J. Kramer, T.Q. Nguyen, and G.C. Bazan, *Adv. Mater.* 26, 2993–2998 (2014).
12. G. Hadziioannou and G. Malliaras, *Semiconducting Polymers* (Weinheim: Wiley-VCH, 2007).
13. Z. Liu, M. Kobayashi, B.C. Paul, Z. Bao, and Y. Nishi, *Phys. Rev. B* 82, 035311–035316 (2010).
14. Y.R. Sun, N.C. Giebink, H. Kanno, B.W. Ma, M.E. Thompson, and S.R. Forrest, *Nature* 440, 908–912 (2006).
15. K.T. Kamtekar, A.P. Monkman, and M.R. Bryce, *Adv. Mater.* 22, 572–582 (2010).
16. B.W. D'Andrade, J. Brooks, V. Adamovich, M.E. Thompson, and S.R. Forrest, *Adv. Mater.* 14, 1032–1036 (2002).
17. S.J. Su, H. Sasabe, T. Takeda, and J. Kido, *Chem. Mater.* 20, 1691–1697 (2008).
18. I. Tanaka, Y. Tabata, and S. Tokito, *Chem. Phys. Lett.* 400, 86–89 (2004).
19. A. Van Dijken, J.J.A.M. Bastiaansen, N.M.M. Kiggen, B.M.W. Langeveld, C. Rothe, A. Monkman, I. Bach, P. Stossel, and K. Brunner, *J. Am. Chem. Soc.* 126, 7718–7727 (2004).
20. K. Brunner, A. Van Dijken, H. Borner, J.J.A.M. Bastiaansen, N.M.M. Kiggen, and B.M.W. Langeveld, *J. Am. Chem. Soc.* 126, 6035–6040 (2004).
21. S.T. Hoffmann, P. Schrögel, M. Rothmann, R.Q. Albuquerque, P. Strohriegl, and A. Köhler, *J. Phys. Chem. B* 115, 414–421 (2011).
22. W. Klöpffer, *Ber. Bunsenges. Phys. Chem.* 73, 864–867 (1969).
23. W. Klöpffer and D. Fischer, *J. Polym. Sci. Polym. Symp.* 40, 43–56 (1973).

24. W. Klöpffer, *ACS Symp. Ser.* 358, 264–285 (1987).
25. G. Rippen, G. Kaufmann, and W. Klöpffer, *Chem. Phys.* 52, 165–177 (1980).
26. A. Itaya, K.I. Okamoto, and S. Kusabayashi, *Bull. Chem. Soc. Jpn.* 49, 2037–2042 (1976).
27. M.T. Vala, J. Haebig, and S.A. Rice, *J. Chem. Phys.* 43, 886–897 (1965).
28. N. Cankaya, E. Tanış, H.E. Gülbaş, and N. Bulut, *Polym. Bull.* 7, 2543–2573 (2019).
29. M. Kurban and B. Gündüz, *J. Phys. Chem. Lett.* 691, 14–21 (2018).
30. C. Orek, B. Gündüz, O. Kaygili, and N. Bulut, *Chem. Phys. Lett.* 678, 130–138 (2017).
31. M.J. Frisch, et al., *Gaussian 09, Revision A.1* (Wallingford: Gaussian Inc, 2009).
32. A.D. Becke, *Phys. Rev. A* 38, 3098–3100 (1988).
33. T. Yanai, D.P. Tew, and N.C. Handy, *Chem. Phys. Lett.* 393, 51–57 (2004).
34. M.J.G. Peach, E.I. Tellgren, P. Salek, T. Helgaker, and D.J. Tozer, *J. Phys. Chem. A* 111, 11930–11937 (2007).
35. A.L. Peter, V.M. Kurt, and P.L. Hans, *J. Chem. Phys.* 130, 194114–194121 (2009).
36. N.M. O'Boyle, A.L. Tenderholt, and K.M. Langner, *J. Comput. Chem.* 29, 839–845 (2008).
37. B. Gündüz, *Polym. Bull.* 72, 3241–3267 (2015).
38. J. Tauc and A. Menth, *J. Non-Cryst. Solids* 569, 8–10 (1972).
39. B. Gündüz, *Opt. Mater.* 3, 425–436 (2013).
40. S.K. Tripathy, *Opt. Mater.* 46, 240–246 (2015).
41. S. Adachi, *Optical Constants of Crystalline and Amorphous Semiconductors* (Dordrecht: Kluwer Academic Publishers, 1999).
42. F. Abeles, *Optical Properties of Solids* (Amsterdam: North-Holland Publishing Company, 1972).
43. B. Gündüz, *Polym. Adv. Technol.* 27, 144–155 (2016).
44. E.B. Sas, E. Tanış, B. Gündüz, and M. Kurt, *Mater. Res. Express* (2020). https://doi.org/10.1088/2053-1591/ab6251.
45. K. Govindarasu and E. Kavitha, *Spectrochim. Acta Part A* 122, 130–141 (2014).
46. K. Govindarasu, E. Kavitha, and N. Sundaraganesan, *Spectrochim. Acta Part A* 133, 417–431 (2014).
47. E. Tanış, E. Babur Şaş, M. Kurban, and M. Kurt, *J. Mol. Struct.* 1154, 301–318 (2017).
48. T. Hughbanks and R. Hoffmann, *J. Am. Chem. Soc.* 105, 3528–3537 (1983).
49. J.G. Małecki, *Polyhedron* 29, 1973–1979 (2010).
50. M. Chen, U.V. Waghmare, C.M. Friend, and E. Kaxiras, *J. Chem. Phys.* 109, 6854–6860 (1998).